
Learning Capacity: A Measure of the Effective Dimensionality of a Model

Daiwei Chen*, Wei-Kai Chang*, Pratik Chaudhari
 University of Pennsylvania
 Email: {daiweic, changwk, pratikac}@seas.upenn.edu
 * Equal Contribution

Abstract

We exploit a formal correspondence between thermodynamics and inference, where the number of samples can be thought of as the inverse temperature, to define a “learning capacity” which is a measure of the effective dimensionality of a model. We show that the learning capacity is a tiny fraction of the number of parameters for many deep networks trained on typical datasets, depends upon the number of samples used for training, and is numerically consistent with notions of capacity obtained from the PAC-Bayesian framework. The test error as a function of the learning capacity does not exhibit double descent. We show that the learning capacity of a model saturates at very small and very large sample sizes; this provides guidelines, as to whether one should procure more data or whether one should search for new architectures, to improve performance. We show how the learning capacity can be used to understand the effective dimensionality, even for non-parametric models such as random forests and k -nearest neighbor classifiers.

1 Introduction

Artificial neural networks have many more parameters than the number of training data. They can therefore overfit, i.e., make inaccurate predictions on data outside the training set. In practice, these networks seem to defy this accepted statistical wisdom and work extremely well across a large class of problems. In practice, the test error often improves as networks with larger and larger numbers of parameters are fitted to the same dataset. This indicates that direct counting of the number of parameters in the network cannot serve as a faithful indicator of the complexity of the model.

This paper discusses a potential solution to this paradox: it develops a quantity called the “learning capacity” to measure the effective dimensionality of a model. It exploits a formal correspondence between statistical inference and thermodynamics, first pointed out by Lamont and Wiggins¹, as follows. Consider a dataset $D = \{(x_i, y_i)\}_{i=1}^N$ where $x \in \mathbb{R}^d$ denotes the input and $y \in \{1, \dots, m\}$ denotes the ground-truth label for m different categories. The probabilistic model of the labels given the input is denoted by $p_w(y | x)$ where $w \in \mathbb{R}^d$ are the weights, or parameters. For every weight configuration w , we can assign a negative energy

$$\hat{H}(w) = -\frac{1}{N} \sum_{i=1}^N \log p_w(y_i | x_i), \quad (1)$$

which is the negative log-likelihood of the training dataset given the weights w , e.g., the cross-entropy loss for classification. If $\varphi(w)$ denotes a prior distribution on the weight space, then the marginal likelihood, also known as the log-partition function in physics or the evidence in statistics, is

$$Z(N) = \int dw \varphi(w) e^{-N\hat{H}(w)}. \quad (2)$$

This expression is quite similar to the expression for the Helmholtz free energy of the constant temperature canonical ensemble² where the probability of finding the system at a state s is given by the Boltzmann distribution

$$\rho(s) \propto \exp(-E(s)/(k_B T));$$

here k_B is the Boltzmann constant, T is the temperature and $E(s)$ is the energy of the state s . The normalizing factor of this distribution is $Z(T) = \int ds e^{-E(s)/(k_B T)}$. The inverse temperature in statistical physics (assuming that we work in natural units with $k_B = 1$) can therefore be considered to be equivalent to the number of samples in statistical inference:

$$\beta = T^{-1} \equiv N. \quad (3)$$

At a small sample size N many weight configurations that are likely under the prior $\varphi(w)$ are consistent with the data; as the number of samples $N \rightarrow \infty$ fewer and fewer weight configurations can fit the data. This allows us to define classical quantities in thermodynamics using their statistical analogues:

$$\begin{aligned} \text{(Average Energy)} \quad U &\doteq -\partial_\beta \log Z(\beta) \equiv -\partial_N \log Z(N), \\ \text{(Capacity)} \quad C &\doteq \beta^2 \partial_\beta^2 \log Z(\beta) \equiv N^2 \partial_N^2 \log Z(N) \\ &= -N^2 \partial_N U. \end{aligned} \quad (4)$$

Both the average energy U and capacity C are functions of the N samples $x^N = (x_1, \dots, x_N)$ in the dataset. We next define their averaged variants \bar{U} , \bar{C} and $\bar{\log Z}$ where $\bar{f} = \mathbb{E}_{x^N} [f]$ for any function f . In the sequel, we will call \bar{U} and \bar{C} , the ‘‘average energy’’ and the ‘‘learning capacity’’ respectively.

Just like the heat capacity of an object is the amount of heat required to produce a unit change in the temperature, the learning capacity of a model is proportional to the drop in the test negative log-likelihood if one additional datum is added to the training dataset.

Contributions:

1. **We develop a procedure to estimate the effective dimensionality of models** ranging from deep networks with different architectures (fully-connected, convolutional and residual) fitted on image classification tasks, to non-parametric models such as random forests and k -nearest neighbor classifiers fitted to tabular datasets. We show that numerical estimates of the learning capacity can be fruitfully used for model selection because it correctly captures trends in the test loss, e.g., for the same sample size, models with a *smaller* learning capacity has a better test loss. We show that the effective dimensionality, as measured by the learning capacity, is a tiny fraction ($\sim 1\%$) of the total number of weights in a model.
2. **We show that the test loss plotted against the learning capacity does not exhibit double descent.** The test loss monotonically increases with the learning capacity for small sample sizes and saturates to a small value for large sample sizes.
3. **We connect the learning capacity to estimates of the effective dimensionality obtained from non-vacuous PAC-Bayes generalization bounds** and show that the two quantities are numerically close to each other, and both are much smaller than the number of weights. We also discuss how the learning capacity is equal to the so-called log-canonical threshold in singular learning theory which characterizes the dimensionality of probabilistic models when there are symmetries in the parameter space.
4. **We show a ‘‘freezing’’ phenomenon in the effective dimensionality of many architectures.** The learning capacity saturates for very small (equivalent to high temperature) and very large (equivalent to low temperature) sample sizes. Different architectures with very different numbers of parameters trained on the same dataset have the same learning capacity for very small sample sizes; this suggests that one should procure more data to improve the test loss in this regime. When the sample size N is large, when the learning capacity freezes, our formulae indicate a regime of diminishing returns where the test loss is proportional to N^{-1} , and our experiments indicate in this regime, one should search for different architectures to improve the test loss—for fixed N , smaller the saturated learning capacity better the test loss.

2 Methods

Even if we have introduced all quantities in the context of classification problems, we can also set up this correspondence for regression. If targets $y_i \in \mathbb{R}$ and if $f_w(x)$ is the prediction on the input x , we can again assign the same energy as that in [1] but with a different probabilistic model:

$\log p_w(y | x) = -\frac{(y - f_w(x))^2}{2\sigma^2} + \text{constant}$, for some non-zero standard-deviation σ . All thermodynamic quantities, in particular the average energy U and the capacity C , can be calculated using the same expressions as those above. Let us also note that the correspondence between thermodynamics and Bayesian inference is not unique. As we discuss in Appendix A, it is useful to use different correspondences depending upon the application.

The Bayesian predictive log-likelihood of a new datum x is

$$\log p(y | x, D) = \log \frac{\int dw p_w(y | x) \varphi(w) e^{-N\hat{H}(w)}}{\int dw \varphi(w) e^{-N\hat{H}(w)}} = \log Z(N+1) - \log Z(N). \quad (5)$$

where in the first step we sent the likelihood of a test datum $p_w(y | x)$ into the exponent. This shows that the average test likelihood of a datum (up to a constant is the entropy of the true labels) is

$$- \mathbb{E}_{x, y \sim P} [\log p(y | x, D)] = \overline{\log Z(N+1)} - \overline{\log Z(N)}. \quad (6)$$

This will be an important identity for us in the sequel because we will estimate quantities like $\overline{\log Z}$ to characterize the test likelihood given by a model.

2.1 Estimating the effective dimensionality of a learned model using PAC-Bayesian framework

The PAC-Bayesian framework^{3,4} estimates the population error of a randomized hypothesis with a distribution Q using its empirical error and its KL-divergence with respect to some prior φ . For any $\delta > 0$, with probability at least $1 - \delta$ over draws of the samples in the training dataset, we have

$$e(Q) \leq \hat{e}(Q) + \sqrt{\frac{\text{KL}(Q, \varphi) + \log(N/\delta)}{2(N-1)}},$$

where $e(Q)$ is the average population error of hypotheses sampled from Q and $\hat{e}(Q)$ is the analogously defined training error. PAC-Bayes theory has been fruitfully used to calculate non-vacuous generalization bounds, even for deep networks^{5,6}. The authors in⁷ showed that if we consider a Gaussian prior $\varphi = \mathcal{N}(w_0, \epsilon^{-1}I)$ for a user-chosen value of ϵ and a Gaussian PAC-Bayes posterior $Q = \mathcal{N}(w, \Sigma_q)$ centered at a fixed weight configuration w (usually taken to be the weights obtained at the end of the training process), then (an upper bound on) the right-hand-side can be optimized analytically. If the Hessian $H(w) \in \mathbb{R}^{p \times p}$ at w is $(H(w))_{ij} = \partial_{w_i} \partial_{w_j} \hat{H}(w)$ for two weights w_i, w_j , then the covariance of the PAC-Bayes posterior $\Sigma_q = U_w (\bar{\Lambda}_w)^{-1} U_w^\top$ where $\bar{\Lambda}_w = \text{diag}(\bar{\lambda}_1, \dots, \bar{\lambda}_p)$ and

$$\bar{\lambda}_i = 2(N-1)\lambda_i + \epsilon \quad (7)$$

where the Hessian is $H(w) = U_w \Lambda_w U_w^\top$ whose eigenvalues are $\Lambda_w = \text{diag}(\lambda_1, \dots, \lambda_p)$ arranged in decreasing order of magnitude and its corresponding eigenvectors are the columns of U_w . It can be shown that for eigenvalues of the Hessian λ_i which are smaller than $\epsilon/(2(N-1))$, the PAC-Bayes posterior spreads its probability mass to reduce the KL-divergence with respect to the prior φ ; in directions where the eigenvalues of the Hessian are larger than this threshold, the spread of the PAC-Bayes posterior Q is determined by how quickly the training loss changes in those directions, and thereby the Hessian. This motivated the authors in⁷ to define

$$p(N, \epsilon) \doteq \sum_{i=1}^p \mathbf{1} \left\{ |\lambda_i| \geq \frac{\epsilon}{2(N-1)} \right\} \quad (8)$$

as the effective dimensionality of a deep network. It is useful to notice that the effective dimensionality $p(N, \epsilon)$ converges to the number of weights p as $N \rightarrow \infty$, i.e., with infinite amounts of data the model uses all its degrees of freedom. The test error can be bounded using

$$e(Q) \leq \frac{\left(\sum_{i=1}^{p(N, \epsilon)} \log \bar{\lambda}_i \right) + 2/\kappa + \epsilon \|w - w_0\|_2^2}{4(N-1)} \quad (9)$$

where κ is the largest constant such that the ratio of the eigenvalues of the Hessian satisfies $\log \lambda_i / \lambda_r = -\kappa(i-r)$ for $r = p(N, \epsilon)$; in other words the eigenvalues decay exponentially quickly after $p(N, \epsilon)$ with slope κ on a logarithmic scale. The authors show that this analytical bound is numerically non-vacuous for fully-connected and convolutional deep networks on MNIST.

2.2 Estimating the effective dimensionality using singular learning theory

A more general version of the above PAC-Bayes calculations, one that does not assume that the posterior Q is Gaussian, can be obtained by directly estimating the free-energy $-N^{-1} \log Z(N)$ corresponding to [2]; this quantity is also known as stochastic complexity. Watanabe⁸ has calculated asymptotic expressions of the stochastic complexity and has shown that

$$-\mathbb{E}_{x^N} [\log Z(N)] = K \log N + \mathcal{O}(\log \log N), \quad (10)$$

where K is the real-log canonical threshold (RLCT) in algebraic geometry that characterizes, roughly speaking, the co-dimension of the model after accounting for symmetries (e.g., permutation symmetries in a neural network) of the weight space. The Fisher Information Metric (FIM) $g(w) \in \mathbb{R}^{p \times p}$ is the metric of the manifold of probability distributions $\{p_w(y | x) : w \in \mathbb{R}^p\}$ parameterized by the weights w and it becomes singular ($\det g(w) = 0$) at these symmetries because there are directions in which the weights can be perturbed without changing the probabilities $p_w(y | x)$. Statistical inference of such models, which includes deep networks, Gaussian mixture models, Bayesian networks with hidden units etc., is the subject of singular learning theory. For models without singularities (also called regular models), e.g., linear regression, the log-canonical threshold is equal to twice the number of parameters, i.e., $K = 2p$ and, in this form [10], is well-known as the Bayes Information Criterion (BIC). In general, the log-canonical threshold is smaller than half the number of parameters for non-regular models. From [5] and [10], we have that, up to a constant is the entropy of the true labels,

$$-\mathbb{E}_{x, y \sim P} [\log p(y | x, D)] = \frac{K}{N} + \mathcal{O}(N^{-1}) \quad (11)$$

asymptotically as $N \rightarrow \infty$. In other words, smaller the log-canonical threshold K , smaller the average test negative log-likelihood.

Remark 1 (The log-canonical threshold measures the number of degrees of freedom that are constrained in a trained model). The following alternative expression provides more intuition:

$$K(w) = \lim_{\epsilon \rightarrow 0} \frac{\log V_w(a\epsilon) - \log V_w(\epsilon)}{\log a} \quad (12)$$

for any $a > 0$ where $V_w(\epsilon)$ is the volume under the prior φ of the sub- ϵ level set of the loss, i.e.,

$$V_w(\epsilon) = \int_0^\epsilon d\epsilon' \int dw \delta_{\epsilon'}(\hat{H}(w)) \varphi(w).$$

This can be understood as the rate at which the logarithm of the number of hypotheses under consideration increases as we allow the training loss, or negative energy $\hat{H}(w)$, to take values that are above the zero loss state (ground state). One way to understand this is to set $\hat{H}(w) = 1$ and $a = e$, i.e., calculate the number of hypotheses without considering their training loss, and see that the limit in [12] is the logarithm of the volume of the shell of thickness $(e - 1)\epsilon$ in p dimensions as the radius of the sphere ϵ goes to zero; this suggests that $K(w) \propto p$.

2.3 Relationship of the average energy and the learning capacity to the test likelihood

Notice that we can write the average energy as $U = \partial_N(NF)$. In statistical physics, this would be written as $U = \partial_\beta \beta F$ for a real-valued β . In our case, the temperature N takes discrete values and we should calculate the finite difference derivative instead. Like Lamont and Wiggins suggest¹, we can reduce the number of samples from N to $(N - 1)$ in N different ways by dropping different samples in the training dataset. An average over these “leave-one-out cross-validation” estimates is a good way to estimate the average energy U . More formally,

$$\begin{aligned} U = \partial_N(NF) &= -\partial_N \log Z(N) = \log Z(N - 1) - \log Z(N) \\ &= -N^{-1} \sum_{i=1}^N \log p(y_i | x_i, D^{(-i)}), \end{aligned} \quad (13)$$

where $D^{(-i)}$ denotes a training dataset of $(N - 1)$ samples with the i^{th} sample removed. In practice, we are interested in estimating U for large datasets and large models, and we will compute averages using the k -fold cross-validation datasets. To summarize, the average energy U is simply the negative log-likelihood on the test datum. Using [13] and [10], we can now show that

$$\bar{C}(N) = K + \mathcal{O}(N^{-1}). \quad (14)$$

Architecture	Dataset	Test Accuracy (%)	Test Loss ($\bar{U}(N)$)	Weights (p)	Learning Capacity ($\bar{C}(N)$)	$\bar{C}(N)/p$ (%)
FC-1-100	MNIST	97.6 \pm 0.1	0.09 \pm 0.01	78,902	609 \pm 560	0.8
LeNet		98.9 \pm 0.1	0.04 \pm 0.01	43,746	231 \pm 204	0.5
ALLCNN	CIFAR-10	88.9 \pm 0.3	0.53 \pm 0.02	262,238	4571 \pm 1700	1.7
Wide-ResNet		93.7 \pm 0.1	0.43 \pm 0.02	298,542	5805 \pm 1145	1.9
Synthetic (κ)						
	0.1	93.7 \pm 0.2	0.20 \pm 0.01		1117 \pm 221	1.4
FC-1-100	1	93.9 \pm 0.2	0.19 \pm 0.01	78,902	870 \pm 338	1.1
	10	98.1 \pm 0.3	0.05 \pm 0.00		112 \pm 39	0.1
	20	98.8 \pm 0.3	0.05 \pm 0.00		70 \pm 19	0.1

Table 1: For different datasets and architectures, the learning capacity $\bar{C}(N)$ at $N = 50,000$ (which is the largest sample size for these datasets) is a very small fraction of the number of weights p (the fraction \bar{C}/p is in percentage). Broadly, larger the complexity of the dataset larger the learning capacity, e.g., CIFAR-10 consists of RGB images while MNIST contains grayscale images, synthetic datasets with a small κ are harder than datasets with a large value of κ . The synthetic data was created by sampling $d = 200$ dimensional inputs from a Gaussian distribution whose covariance has eigenvalues that decay as $\lambda_i = e^{-\kappa i}$ (i.e., larger the slope κ , more low-dimensional the inputs and smaller the PAC-Bayes bound in [9]) and labeling these inputs using a random teacher network with one hidden layer. The learning capacity of trained student networks on such data is remarkably small.

In other words, the learning capacity is proportional to the log-canonical threshold which characterizes the number of degrees of freedom that are constrained in the trained model and thereby controls the negative test log-likelihood (see [11]).

Appendix B discusses how to numerically estimate the learning capacity. We have also developed an alternative expression to estimate \bar{U} and \bar{C} using Markov chain Monte Carlo methods in Appendix B.1.

3 Results

We investigated the concepts developed above using different types of models, multi-layer perceptrons, convolutional networks (LeNet⁹ and ALLCNN¹⁰), residual¹¹ and wide-residual networks¹² and also classifiers that do not maintain a representation of the parameters such as random forests and k -nearest neighbor classifiers. We trained these models under different settings on MNIST⁹, CIFAR-10¹³, synthetic datasets of varying degrees of complexity, and also multiple tabular datasets. Appendix C provides more details*.

3.1 The learning capacity for deep neural networks (a) is a tiny fraction of the number of weights, (b) increases with the number of samples and complexity of the training data, and (c) exhibits freezing at very small and very large sample sizes.

Table 1 shows the learning capacity for different architectures trained on different datasets and a comparison with the number of weights in each architecture. In all cases, the learning capacity \bar{C} at the maximum sample size of these datasets ($N = 50,000$) is a tiny fraction of the number of weights. This indicates a large degree of redundancy in how the weights are used to make predictions. This observation is consistent with many results in physics and systems biology where this has been studied under the name of “sloppy models”^{14–16}, and also with results in deep learning, e.g., the lottery ticket hypothesis^{17,18}. The

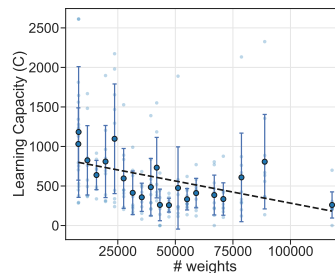


Figure 1: Learning capacity as a function of the number of weights for different fully-connected networks with one to two hidden layers trained on MNIST; each solid dot represents the average of 10 networks and error bars represent one standard deviation. The capacity is a small fraction of the number of weights and decreases slightly with the number of weights; a linear regression has slope of -0.006 ± 0.002 (95% confidence).

*In order to compare with existing PAC-Bayes-based generalization bounds, we have estimated the learning capacity for a binary classification problem on MNIST (even digits vs. odd digits). For the same reason, we do not use any data augmentation during training for any of the datasets.

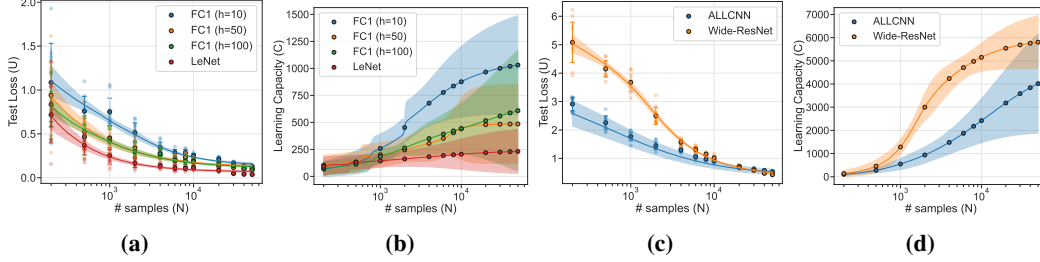


Figure 2: (a,c) show the estimate of the average energy $\bar{U}(N)$ for different architectures, for MNIST and CIFAR-10 respectively. In general, the average energy decreases monotonically as a function of the number of samples N in the training dataset. For MNIST, the convolutional network (LeNet) achieves the best test loss while the ALLCNN network achieved a smaller test loss for CIFAR-10 for most sample sizes except very large ones where the Wide-ResNet has a smaller loss (no data augmentation was used in these experiments); see Table 1 for the error. (b,d) show the estimate of the learning capacity $\bar{C}(N)$ as a function of N . The learning capacity, which indicates the number of constrained degrees of freedom in a model, increases as the number of training samples increases. Different architectures trained on the same dataset have different learning capacity. For both MNIST and CIFAR-10, architectures with a smaller learning capacity (LeNet and ALLCNN respectively) have the smaller test loss. The learning capacity exhibits freezing at both very small and very large N .

learning capacity, like the log-canonical threshold in [12], is a measure of the number of constrained degrees of freedom and this result suggests very few degrees of freedom are constrained by the data in these models. In Fig. 1, the learning capacity for many different fully-connected networks trained on MNIST decreases slightly as a function of the number of weights p in the architecture. We speculate that this is due to the difficulty of training larger networks.

Fig. 2 shows the estimates of the average energy $\bar{U}(N)$ and the learning capacity $\bar{C}(N)$ for different deep networks trained on MNIST and CIFAR-10 datasets for different sample sizes N . As expected from learning theory, the average energy (test loss) decreases monotonically with N . Different architectures trained have different learning capacities but, unlike that of learning theory, the same architecture has different capacities at different sample sizes. In Fig. 3 we show the test loss and learning capacity for fully-connected student networks fitted on datasets of varying degrees of complexity labeled by a fixed random teacher. Inputs of these datasets are sampled from a Gaussian with zero mean and a covariance matrix whose eigenvalues decay exponentially with different slopes; larger the slope, smaller the effective rank of the dataset and more effectively low-dimensional the true model. The learning capacity tracks this trend well, it is large when inputs are not effectively low-dimensional.

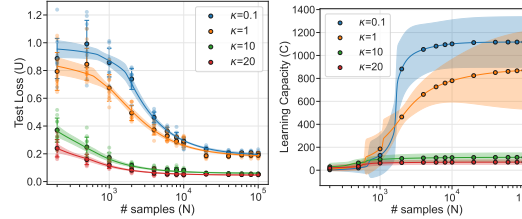


Figure 3: Average energy \bar{U} (left) and learning capacity \bar{C} (right) for fully-connected student networks with one hidden layer (100 neurons) fitted on synthetic datasets of varying degrees of complexity labeled by a one-hidden layer random teacher (1000 neurons). At large N , smaller the coefficient κ , larger the complexity (see [9]) and larger the learning capacity; at small N all networks have the same capacity.

Susceptibilities in thermodynamics (e.g., heat capacity or bulk modulus) quantify the changes in an extensive property (e.g., the average energy) under variations of an intensive property (e.g., the temperature) and are very useful to systematically characterize materials. Our results suggest that some architectures are better suited to some datasets than others, e.g., even if the wide residual network is both bigger and regarded to be “better” than ALLCNN, the latter may be better suited for some problems in terms of how quickly the test loss decreases with the number of samples. While the test loss/error of all the models on MNIST is quite similar at large sample sizes, the convolutional network is using very few degrees of freedom to make accurate predictions.

All networks in Fig. 2 exhibit a freezing phenomenon where the learning capacity saturates at very high or very low sample sizes (except ALLCNN at large N). Different architectures have the same capacity at small sample sizes; this suggests that when the amount of information in the training dataset is small, a small fraction of the degrees of freedom is constrained. This is a validation of our

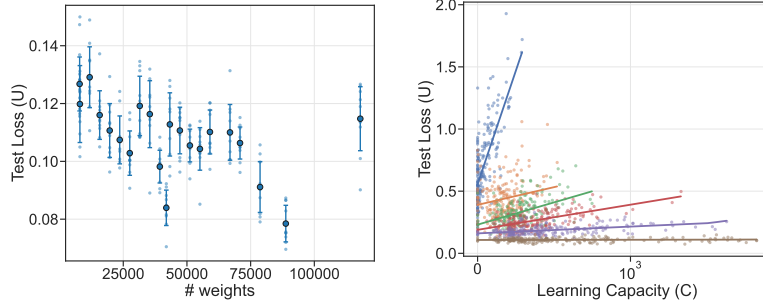


Figure 4: **Left:** a double descent phenomenon for the test loss as a function of the number of weights for one and two-layer fully-connected networks with different numbers of hidden neurons (10–100) trained on MNIST with sample size $N = 50,000$. **Right:** the test loss as function of the learning capacity for same architectures for different values of N (blue: 200, orange: 1000, green: 2000, red: 4000, purple: 10000, and brown: 50,000) does not exhibit double descent. The slope of all regressions is non-zero and positive with statistically significant $p < 0.005$ except the brown curve for which the p -value of the slope being non-zero is not significant.

definition of learning capacity. The architectures have different capacities at large N , but smaller the capacity better the test loss. When N is large \bar{U} decreases as $\approx 1/N$ if \bar{C} is constant. This suggests that we should search for different architectures in this regime when there are diminishing returns from increasing N .

3.2 Test loss as a function of the learning capacity does not exhibit double descent

The double descent phenomenon¹⁹, where the test error decreases as models with more parameters are fitted upon the data, suggests that the classical bias-variance trade-off may not hold as-is for deep networks. There is an extensive literature on this topic^{20,21} but we do not have a way to reconcile the classical U-shaped curve in the bias-variance tradeoff with the monotonic decrease of test error in deep networks. Fig. 4 shows the test loss as a function of the learning capacity for a large variety of networks (fully-connected networks with number of hidden neurons ranging from 10 to 100 trained on MNIST using samples ranging from $N = 200$ to $N = 50,000$ each shown in a different color) and contrasts this with the double descent curve for $N = 50,000$. In all cases, the slope of a regression fitted to the test loss (equivalent to average energy \bar{U}) as a function of the learning capacity \bar{C} is positive (except for $N = 50,000$ where the p -value for the slope being non-zero is not significant). This is a strong validation of the fact that learning capacity can adequately measure the complexity of a learned model. Indeed a good metric of complexity should be positively correlated with the test loss. This is also a reassurance that even in deep learning, we should select models with a smaller complexity to obtain a small test loss—not necessarily a small number of weights but a small learning capacity.

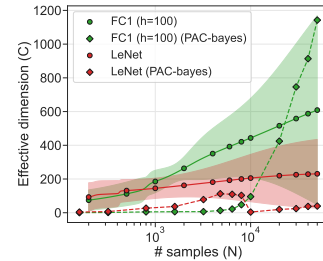


Figure 5: The learning capacity \bar{C} (solid lines) is consistent with an estimate of the effective dimensionality of a deep network [8] obtained by optimizing the posterior in a PAC-Bayes bound (dotted lines).

3.3 Learning capacity is consistent with the effective dimensionality obtained from PAC-Bayes theory

We next compare our estimates of the learning capacity with the expression for the effective dimensionality in⁷, which we have discussed in [8]. Computing this expression involves solving for the eigenvalues of the Hessian of trained network, which we do using a Kronecker-decomposition of the block-diagonal Hessian using Backpack²², and optimizing the posterior in the right hand-side of the PAC-Bayes bound numerically to compute the best scale ϵ for the prior $\varphi = \mathcal{N}(w_0, \epsilon^{-1}I)$. Doing so correctly to calculate good PAC-Bayes bounds is delicate, we defer to⁷ for the details of the optimization. As Fig. 5 shows, our estimates for learning capacity are of the same order as the effective dimensionality estimated from PAC-Bayes theory—and both are much smaller than the number of parameters in the network. This lends credence to our definition of the learning capacity.

The learning capacity and the PAC-Bayes-based estimate of the effective dimensionality were calculated in very different ways, e.g., the former trained models independently on different folds

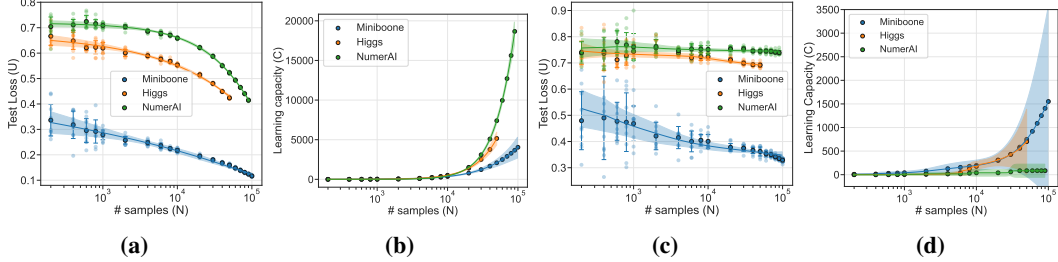


Figure 6: (a,c) show the average energy \bar{U} as a function of the sample size N for three tabular learning datasets for a random forest and k -nearest neighbor classifier respectively. (b,d) show the learning capacity for the random forest and k -nearest neighbor classifier respectively. In both cases, the Miniboone dataset has the best test loss and both models exhibit a lower learning capacity for this dataset (for the k -NN there is a large uncertainty in the estimate in this case). As the random forest learns the Numerai dataset, its capacity (which is reflective of the number of constrained degrees of freedom) increases sharply; in contrast the k -NN does not have a good test loss on this dataset and its capacity is much smaller.

of data whereas the latter optimized the posterior Q centered at a trained network; the former did not optimize the prior from which weights were sampled while beginning training and the latter explicitly optimized the prior to get a tighter bound, etc. The fact that the two quantities are consistent with each other therefore also validates our procedure to compute the learning capacity. We should emphasize that optimizing PAC-Bayes bounds numerically is very challenging technically and, to our knowledge, implementations on datasets that are more complicated than MNIST have not yielded non-vacuous bounds. In contrast, the learning capacity is much more straight-forward to compute.

3.4 Effective dimensionality of non-parametric classifiers

Our technique to estimate the learning capacity is very general and does not require the model to have a representation of its parameters. In order to demonstrate this, we considered two canonical non-parametric classifiers, a random forest and a k -nearest neighbor classifier and fit these models on three tabular datasets. As Fig. 10 shows we can obtain consistent estimates of the capacity in both cases, i.e., for both classifiers, for the same number of samples, datasets where the learning capacity is large also have a larger test loss. We again see a freezing at small sample sizes where the learning capacity is the same for all datasets. Both classifiers trained on most common tabular datasets do not exhibit freezing at large sample sizes: this shows the powerful fitting ability of these adaptive non-parametric methods. For random forests, we can easily have situations where the number of leaves is as large as 10^7 . The VC-dimension of a decision tree is proportional to the number of leaves²³, so such models are also highly over-parameterized when they are fitted on fewer samples than the number of leaves. As we show in Fig. 7, the learning capacity is typically much smaller than the number of leaves irrespective of the dataset—by about 3 orders of magnitude, which is quite consistent with the ratio of \bar{C}/p in Table 1 for deep networks.

This is a remarkable finding because models such as random forests and k -NNs do not have a well-defined objective that is optimized or even a weight space; due to this the PAC-Bayes-based estimation of the effective dimensionality or the log-canonical threshold cannot be defined for these models. It is unclear to us, as yet, what our calculation of the learning capacity for such non-parametric models entails. But this experiment does reinforce the point that the learning capacity is a very general quantity and can be calculated for any predictive method.

4 Discussion and Related Work

Although there is extensive work on model selection in both information theory^{24–26} and machine learning^{27,28}, performing effective model selection for deep networks has been difficult²⁹. The

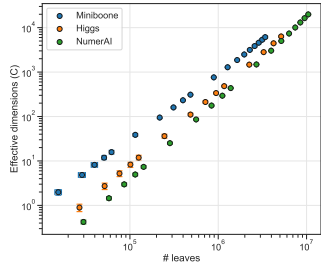


Figure 7: The learning capacity is much smaller (about 0.1%) than the number of leaves in a random forest for all three tabular learning datasets considered here. The capacity also increases monotonically as the number of leaves grows.

key issue is that the number of weights in a deep network do not directly relate to the complexity of the learned model, even if estimates of the VC dimension suggest that the complexity of the hypothesis class is proportional to the number of weights³⁰. Many quantities have been proposed to capture this discrepancy, e.g., to estimate the complexity of the hypothesis class^{31–34}, or that of the learned model^{35–39}. These quantities are often formulated outside our Bayesian framework but there similarities, e.g., compression bounds use perturbations of the input, flatness-based metrics perturb the weight space, while the learning capacity perturbs the number of samples.

Even if deep networks were to be trained with plentiful data, there would still be anomalies in the number of parameters and the complexity of the learned function purely because of the hierarchical architecture. This is because, for singular models such as deep networks, there are many symmetries in the weight space and multiple weight configurations map to the same predictions⁴⁰. Geodesics of the manifold of probability distributions accumulate near such singularities and therefore the training dynamics can slow down enormously^{41,42}. Building upon classical results in statistics⁴³, Watanabe has developed a sophisticated theoretical framework based on algebraic geometry to characterize the statistical properties of such singular models. In a different context, it has been noticed that regression models fitted to data from systems biology are “sloppy”, i.e., they have few number of tightly constrained stiff parameters and a large number of poorly constrained parameters that do not affect predictions much^{15,44}. These ideas have also been used to study deep networks and have provided novel insights into the geometry of the hypothesis space of deep networks^{7,45,46}. Singular learning theory and sloppy models rely on calculating the log-canonical threshold and the Fisher Information Metric to characterize the underlying model—and for modern deep networks trained on large datasets these quantities are rather daunting to compute. The learning capacity discussed here can be used to capture the same concepts and apply them in practice, but it is much easier to compute.

There is an extensive body of theoretical work that studies the double descent phenomenon¹⁹, e.g., using two-layer networks^{47,48}, linear models⁴⁹. The double descent phenomenon is surprising for two reasons: the sharp increases in the variance of the estimator near the interpolation threshold and the monotonic decrease in the test error as the number of parameters in the model grows. The former can be eliminated by regularization⁵⁰ but to our knowledge this paper presents the first demonstration that the latter can also be addressed. Our results show that at small sample sizes, when the test loss is plotted against the learning capacity the test loss grows with increasing capacity—this is akin to the later half of the classic U-shaped curve in the bias-variance tradeoff. For large sample sizes, the test loss saturates as a function of the learning capacity—this indicates that the learning capacity adequately captures the effective dimensionality of the model and even if the number of bare parameters in the hypothesis class grows, the number of degrees of freedom that are constrained by the data does not grow.

For perceptron-like models, calculations in statistical physics^{8,51,52} show that the generalization error (akin to our \bar{U}) is inversely proportional to the sample size N , e.g., $0.625d/N$ and $0.442d/N$ for the so-called Gibbs and Bayes learning rules respectively. The “effective dimensionality” of these rules can be calculated using [4] also saturates at large N . Such insensitivity of the performance to the number of samples has also been noticed in the so-called “deep bootstrap” phenomenon⁵³; this has also been studied theoretically using kernel gradient flows^{54,55}. Our results show a more refined phenomenon: the learning capacity, which is a good estimate of the test loss, saturates at both small and high sample sizes and a sharp transition in between.

Guidelines for using the learning capacity in practice, limitations and perspectives The learning capacity can be estimated using a cross-validation like procedure to calculate the derivative of the test loss with respect to the number of samples; one can estimate the saturation of the capacity using the second derivative to obtain crisp guidelines as to whether one should invest in procuring more data or whether test error would improve if the hypothesis class were chosen differently. It is being noticed that large models are significantly undertrained as a consequence of increasing the number of parameters without increasing the number of samples in the training dataset⁵⁶, and the learning capacity could be a good way to investigate this issue.

The number of weights in deep network is often used for comparison and benchmarking different techniques. While it is broadly appreciated that conclusions can be confounded by how well different models are trained, this practice persists, perhaps due to the lack of an alternative metric. The learning capacity is more expensive to compute for such applications but it could be a sound alternative for benchmarking purposes. Model selection for architectures such as random forests and k -nearest neighbors which do not explicitly represent parameters has not been investigated

before—cross-validation is the method of choice for such architectures. The learning capacity offers an alternative and a very practical way to perform model selection for these classifiers.

5 Acknowledgments

DC and PC were supported by grants from the National Science Foundation (IIS-2145164, CCF-2212519), Office of Naval Research (N00014-22-1-2255), and cloud computing credits from Amazon Web Services. The authors would also like to thank Rubing Yang and Alexander Alemi for their feedback on these ideas.

References

- [1] C. H. LaMont and P. A. Wiggins, “On the correspondence between thermodynamics and inference,” *Physical Review E*, vol. 99, p. 052140, May 2019.
- [2] J. P. Sethna, *Statistical Mechanics: Entropy, Order Parameters, and Complexity*. No. 14 in Oxford Master Series in Statistical, Computational, and Theoretical Physics, 2006.
- [3] J. Langford and M. Seeger, “Bounds for averaging classifiers,” 2001.
- [4] D. A. McAllester, “PAC-Bayesian model averaging,” in *Proceedings of the Twelfth Annual Conference on Computational Learning Theory*, pp. 164–170, 1999.
- [5] G. K. Dziugaite and D. M. Roy, “Computing Nonvacuous Generalization Bounds for Deep (Stochastic) Neural Networks with Many More Parameters than Training Data,” in *Proc. of the Conference on Uncertainty in Artificial Intelligence (UAI)*, 2017.
- [6] Y. Wu, X. Zhu, C. Wu, A. Wang, and R. Ge, “Dissecting Hessian: Understanding Common Structure of Hessian in Neural Networks,” *arXiv:2010.04261 [cs, stat]*, June 2021.
- [7] R. Yang, J. Mao, and P. Chaudhari, “Does the data induce capacity control in deep learning?,” in *Proc. of International Conference of Machine Learning (ICML)*, 2022.
- [8] S. Watanabe, *Algebraic Geometry and Statistical Learning Theory*. No. 25, 2009.
- [9] Y. LeCun, B. E. Boser, J. S. Denker, D. Henderson, R. E. Howard, W. E. Hubbard, and L. D. Jackel, “Handwritten digit recognition with a back-propagation network,” in *Advances in Neural Information Processing Systems*, pp. 396–404, 1990.
- [10] J. T. Springenberg, A. Dosovitskiy, T. Brox, and M. Riedmiller, “Striving for Simplicity: The All Convolutional Net,” *arXiv:1412.6806 [cs]*, Apr. 2015.
- [11] K. He, X. Zhang, S. Ren, and J. Sun, “Identity mappings in deep residual networks,” *arXiv:1603.05027*, 2016.
- [12] S. Zagoruyko and N. Komodakis, “Wide residual networks,” in *British Machine Vision Conference 2016*, 2016.
- [13] A. Krizhevsky, *Learning Multiple Layers of Features from Tiny Images*. PhD thesis, Computer Science, University of Toronto, 2009.
- [14] J. J. Waterfall, F. P. Casey, R. N. Gutenkunst, K. S. Brown, C. R. Myers, P. W. Brouwer, V. Elser, and J. P. Sethna, “Sloppy-Model Universality Class and the Vandermonde Matrix,” *Physical Review Letters*, vol. 97, p. 150601, Oct. 2006.
- [15] K. S. Brown, C. C. Hill, G. A. Calero, C. R. Myers, K. H. Lee, J. P. Sethna, and R. A. Cerione, “The statistical mechanics of complex signaling networks: Nerve growth factor signaling,” *Physical biology*, vol. 1, no. 3, p. 184, 2004.
- [16] R. N. Gutenkunst, J. J. Waterfall, F. P. Casey, K. S. Brown, C. R. Myers, and J. P. Sethna, “Universally sloppy parameter sensitivities in systems biology models,” *PLoS Computational Biology*, vol. 3, no. 10, p. e189, 2007.

- [17] J. Frankle and M. Carbin, “The Lottery Ticket Hypothesis: Finding Sparse, Trainable Neural Networks,” *arXiv:1803.03635 [cs]*, Mar. 2019.
- [18] P. Molchanov, S. Tyree, T. Karras, T. Aila, and J. Kautz, “Pruning convolutional neural networks for resource efficient inference,” in *5th International Conference on Learning Representations, ICLR 2017-Conference Track Proceedings*, 2019.
- [19] M. Belkin, D. Hsu, S. Ma, and S. Mandal, “Reconciling modern machine-learning practice and the classical bias–variance trade-off,” *Proceedings of the National Academy of Sciences*, vol. 116, no. 32, pp. 15849–15854, 2019.
- [20] P. L. Bartlett, A. Montanari, and A. Rakhlin, “Deep learning: A statistical viewpoint,” *Acta Numerica*, vol. 30, pp. 87–201, 2021.
- [21] P. Nakkiran, G. Kaplun, Y. Bansal, T. Yang, B. Barak, and I. Sutskever, “Deep Double Descent: Where Bigger Models and More Data Hurt,” *arXiv:1912.02292 [cs, stat]*, Dec. 2019.
- [22] F. Dangel, F. Kunstner, and P. Hennig, “BackPACK: Packing more into backprop,” in *International Conference on Learning Representations*, 2020.
- [23] J.-S. Leboeuf, F. LeBlanc, and M. Marchand, “Decision trees as partitioning machines to characterize their generalization properties,” *Advances in Neural Information Processing Systems*, vol. 33, pp. 18135–18145, 2020.
- [24] J. Rissanen, “Modeling by shortest data description,” *Automatica*, vol. 14, no. 5, pp. 465–471, 1978.
- [25] A. R. Barron and T. M. Cover, “Minimum complexity density estimation,” *IEEE transactions on information theory*, vol. 37, no. 4, pp. 1034–1054, 1991.
- [26] V. Balasubramanian, “Statistical Inference, Occam’s Razor, and Statistical Mechanics on the Space of Probability Distributions,” *Neural Computation*, vol. 9, pp. 349–368, Feb. 1997.
- [27] B. Schölkopf and A. J. Smola, *Learning with Kernels*. 2002.
- [28] J. Friedman, T. Hastie, and R. Tibshirani, *The Elements of Statistical Learning*, vol. 1. 2001.
- [29] C. Zhang, S. Bengio, M. Hardt, B. Recht, and O. Vinyals, “Understanding deep learning requires rethinking generalization,” in *International Conference on Learning Representations (ICLR)*, 2017.
- [30] P. L. Bartlett, D. J. Foster, and M. J. Telgarsky, “Spectrally-normalized margin bounds for neural networks,” in *Advances in Neural Information Processing Systems*, pp. 6240–6249, 2017.
- [31] T. Liang, T. Poggio, A. Rakhlin, and J. Stokes, “Fisher-rao metric, geometry, and complexity of neural networks,” in *The 22nd International Conference on Artificial Intelligence and Statistics*, pp. 888–896, 2019.
- [32] B. Neyshabur, Y. Wu, R. Salakhutdinov, and N. Srebro, “Path-normalized optimization of recurrent neural networks with ReLU activations,” in *NIPS*, 2016.
- [33] T. Poggio, A. Banburski, and Q. Liao, “Theoretical issues in deep networks,” *Proceedings of the National Academy of Sciences*, vol. 117, pp. 30039–30045, Dec. 2020.
- [34] K. Sun and F. Nielsen, “Lightlike Neuromanifolds, Occam’s Razor and Deep Learning,” *arXiv:1905.11027 [cs, stat]*, Feb. 2020.
- [35] Y. Jiang, B. Neyshabur, H. Mobahi, D. Krishnan, and S. Bengio, “Fantastic generalization measures and where to find them,” in *International Conference on Learning Representations*, 2019.
- [36] R. Shwartz-Ziv and N. Tishby, “Opening the Black Box of Deep Neural Networks via Information,” *arXiv:1703.00810 [cs]*, Apr. 2017.

- [37] A. Achille and S. Soatto, “Where is the Information in a Deep Neural Network?,” *arXiv:1905.12213 [cs, math, stat]*, June 2019.
- [38] S. Hochreiter and J. Schmidhuber, “Flat minima,” *Neural Computation*, vol. 9, no. 1, pp. 1–42, 1997.
- [39] P. Chaudhari, A. Choromanska, S. Soatto, Y. LeCun, C. Baldassi, C. Borgs, J. Chayes, L. Sagun, and R. Zecchina, “Entropy-SGD: Biasing gradient descent into wide valleys,” in *Proc. of International Conference of Learning and Representations (ICLR)*, 2017.
- [40] S. Watanabe, “Almost all learning machines are singular,” in *2007 IEEE Symposium on Foundations of Computational Intelligence*, pp. 383–388, 2007.
- [41] S.-i. Amari, T. Ozeki, R. Karakida, Y. Yoshida, and M. Okada, “Dynamics of Learning in MLP: Natural Gradient and Singularity Revisited,” *Neural Computation*, vol. 30, pp. 1–33, Jan. 2018.
- [42] M. K. Transtrum, B. B. Machta, and J. P. Sethna, “The geometry of nonlinear least squares with applications to sloppy models and optimization,” *Physical Review E*, vol. 83, p. 036701, Mar. 2011.
- [43] D. Dacunha-Castelle and E. Gassiat, “Testing in locally conic models, and application to mixture models,” *ESAIM: Probability and Statistics*, vol. 1, pp. 285–317, 1997.
- [44] R. Gutenkunst, *Sloppiness, Modeling, and Evolution in Biochemical Networks*. PhD thesis, Cornell University, 2007.
- [45] J. Mao, I. Griniasty, H. K. Teoh, R. Ramesh, R. Yang, M. Transtrum, J. P. Sethna, and P. Chaudhari, “The Training Process of Many Deep Networks Explores the Same Low-Dimensional Manifold,” *arXiv preprint arXiv:2305.01604*, 2022.
- [46] R. Ramesh, J. Mao, I. Griniasty, R. Yang, H. K. Teoh, M. Transtrum, J. Sethna, and P. Chaudhari, “A picture of the space of typical learnable tasks,” in *Proc. of International Conference of Machine Learning (ICML)*, 2022.
- [47] S. Mei and A. Montanari, “The generalization error of random features regression: Precise asymptotics and the double descent curve,” *Communications on Pure and Applied Mathematics*, vol. 75, no. 4, pp. 667–766, 2022.
- [48] S. Mei, T. Misiakiewicz, and A. Montanari, “Generalization error of random feature and kernel methods: Hypercontractivity and kernel matrix concentration,” *Applied and Computational Harmonic Analysis*, vol. 59, pp. 3–84, 2022.
- [49] T. Hastie, A. Montanari, S. Rosset, and R. J. Tibshirani, “Surprises in High-Dimensional Ridgeless Least Squares Interpolation,” *arXiv:1903.08560 [cs, math, stat]*, Nov. 2019.
- [50] P. Nakkiran, P. Venkat, S. Kakade, and T. Ma, “Optimal regularization can mitigate double descent,” *arXiv preprint arXiv:2003.01897*, 2020.
- [51] A. Engel and C. V. den Broeck, *Statistical Mechanics of Learning*. Mar. 2001.
- [52] C. Baldassi, A. Ingrosso, C. Lucibello, L. Saglietti, and R. Zecchina, “Subdominant dense clusters allow for simple learning and high computational performance in neural networks with discrete synapses,” *Physical review letters*, vol. 115, no. 12, p. 128101, 2015.
- [53] P. Nakkiran, B. Neyshabur, and H. Sedghi, “The deep bootstrap framework: Good online learners are good offline generalizers,” *arXiv preprint arXiv:2010.08127*, 2020.
- [54] N. Ghosh, S. Mei, and B. Yu, “The three stages of learning dynamics in high-dimensional kernel methods,” *arXiv preprint arXiv:2111.07167*, 2021.
- [55] J. B. Simon, M. Dickens, and M. R. DeWeese, “Neural tangent kernel eigenvalues accurately predict generalization,” *CoRR*, vol. abs/2110.03922, 2021.

- [56] J. Hoffmann, S. Borgeaud, A. Mensch, E. Buchatskaya, T. Cai, E. Rutherford, D. d. L. Casas, L. A. Hendricks, J. Welbl, A. Clark, *et al.*, “Training compute-optimal large language models,” *arXiv preprint arXiv:2203.15556*, 2022.
- [57] P. Chaudhari and S. Soatto, “Stochastic gradient descent performs variational inference, converges to limit cycles for deep networks,” in *Proc. of International Conference of Learning and Representations (ICLR)*, 2018.
- [58] M. Newville, T. Stensitzki, D. B. Allen, and A. Ingargiola, “LMFIT: Non-Linear Least-Square Minimization and Curve-Fitting for Python,” Sept. 2014.
- [59] M. Welling and Y. W. Teh, “Bayesian learning via stochastic gradient Langevin dynamics,” in *ICML*, pp. 681–688, 2011.
- [60] G. E. Crooks, “Measuring thermodynamic length,” *Physical Review Letters*, vol. 99, p. 100602, Sept. 2007.
- [61] R. Fakoor, J. Mueller, N. Erickson, P. Chaudhari, and A. J. Smola, “Fast, accurate, and simple models for tabular data via augmented distillation,” in *Proc. of Conference on Neural Information Processing Systems (NeurIPS)*, 2020.
- [62] L. N. Smith and N. Topin, “Super-Convergence: Very Fast Training of Neural Networks Using Large Learning Rates,” *arXiv:1708.07120 [cs, stat]*, May 2018.

A Is the analogy between thermodynamics and statistical inference unique?

There have been other attempts to explore similarities between thermodynamics and Bayesian inference. For example, a continuous-time model of stochastic gradient descent (SGD) as a Langevin dynamics with state-dependent noise is

$$dw(t) = -\nabla \hat{H}(w) dt + \left(\frac{\eta}{N_0} D(w) \right)^{1/2} dB(t)$$

where $\nabla \hat{H}(w)$ is the gradient of the training objective (cross-entropy loss), $\eta > 0$ is the step-size or learning rate of SGD, $N_0 < N$ is the mini batch-size, $D(w) = \text{Cov}(\nabla \hat{H}(w))$ is the covariance of the mini-batch gradient and $B(t)$ is standard Brownian motion⁵⁷. We can think of the factor η/N_0 as a temperature; larger the learning rate larger the effective noise in the SGD weight updates as compared to gradient descent, and larger the mini-batch size N_0 smaller the discrepancies between the SGD gradient and the full gradient. Indeed, for this model, with some technical assumptions, the probability density over the weight space ρ^* induced by SGD can be shown to be

$$\rho^*(w) = \underset{\rho}{\operatorname{argmin}} \mathcal{F}(\rho) := \left\{ \mathbb{E}_{w \sim \rho} [\Phi(w)] - \frac{\eta}{N_0} H(\rho) \right\}$$

where $H(\rho) = -\int dw \rho(w) \log \rho(w)$ is the Shannon entropy of the density ρ and the first term is like an average energy where the function $\Phi(w)$ gets minimized on average over draws of weights from the probability density ρ^* . For this setup, the free energy is $\mathcal{F}(\rho)$, the temperature is η/N_0 and the updates of SGD can be understood as performing Bayesian inference using a uniform prior over the weight space, i.e., where the Kullback-Leibler divergence $\text{KL}(\rho, \varphi) = H(\rho)$ when φ is uniform, say on a compact set.

The analogy above regarding SGD is useful to understand the steady-state distribution using non-equilibrium thermodynamics⁵⁷. The correspondence used in this paper is useful to understand generalization. A yet another variant is found in Watanabe’s work which uses a different definition of Bayesian inference in his development of singular learning theory⁸. He studies situations when the likelihood term in Bayes law $p_w(y | x)$ is modified to be $p_w^\beta(y | x)$ for an arbitrary power β . This is useful for the purposes of numerically calculating Bayesian posteriors, e.g., using Markov chain Monte Carlo methods, because the posterior is continuous in this new inverse temperature β . But this changes the definitions of the average energy and it no longer corresponds to the test negative log-likelihood.

The analogy between thermodynamics and statistical inference is not unique. Which one we use, and to what extent, depends upon the application.

B Numerical estimates of thermodynamic quantities

For each model class and dataset, e.g., different deep networks, random forests and different datasets, we perform the following steps to first estimate the average energy (averaged over multiple sample sets) $\bar{U}(N)$.

- For each value of N , sub-sample n different datasets $D_N^{(i)} \subseteq D$ for $i \in \{1, \dots, n\}$ with replacement (i.e., bootstrapped versions of the datasets), each with N samples.
- Create k -folds within each dataset $D_N^{(i)}$ and for each fold. Let the j^{th} fold be $\xi^{(j)} \subset D_N^{(i)}$; this has $(1 - 1/k)N$ samples in the training set and N/k samples in the test set. For each fold, train m models, say denoted by parameters $w^{(l)}$; $l \in \{1, \dots, m\}$ from different initializations (random seeds in practice) and calculate

$$\bar{U}(N) = -\frac{1}{nmN} \sum_{i=1}^n \sum_{j=1}^k \sum_{(x,y) \in \xi^{(j)} \subset D_N^{(i)}} \sum_{l=1}^m \log p_{w^{(l)}}(y | x) \quad (15)$$

The normalization does not depend on k because the k -dependent factor from averaging over N/k samples in the test set of each fold cancels out with the factor of $1/k$ coming from averaging over the k folds. For all experiments, we set the the number of bootstrapped datasets $n = 4$, the number of folds $k = 5$, and the number of different models trained on each fold $m = 5$. For each value of N (we roughly use 15 values; close by at small sample sizes and far apart for large sample sizes), this amounts to training 100 models to estimate \bar{U} .

Given these estimates of the average energy, we could now calculate $\bar{C} = -N^2 \partial_N \bar{U}$ but it is difficult to do so because the noise in the estimation of \bar{U} gets amplified when we take the finite-difference derivative. Therefore in preliminary experiments, we used a polynomial model to fit $\bar{U}(N)$ (with the constraint that it decreases monotonically with N ...since it is akin to the test loss) and calculated the analytical derivative of this polynomial to obtain an estimate of $\bar{C}(N)$; note that this procedure can also give an estimate of the uncertainty on both \bar{U} and \bar{C} . As shown in Fig. 8, this works reasonably well but has a large uncertainty in the estimated value of \bar{C} . We also noticed that—in all cases—the learning capacity \bar{C} as a function of the number of samples N looked like a sigmoid, i.e., it saturated at both very small and very large sample sizes with a sharp rise at some intermediate value.

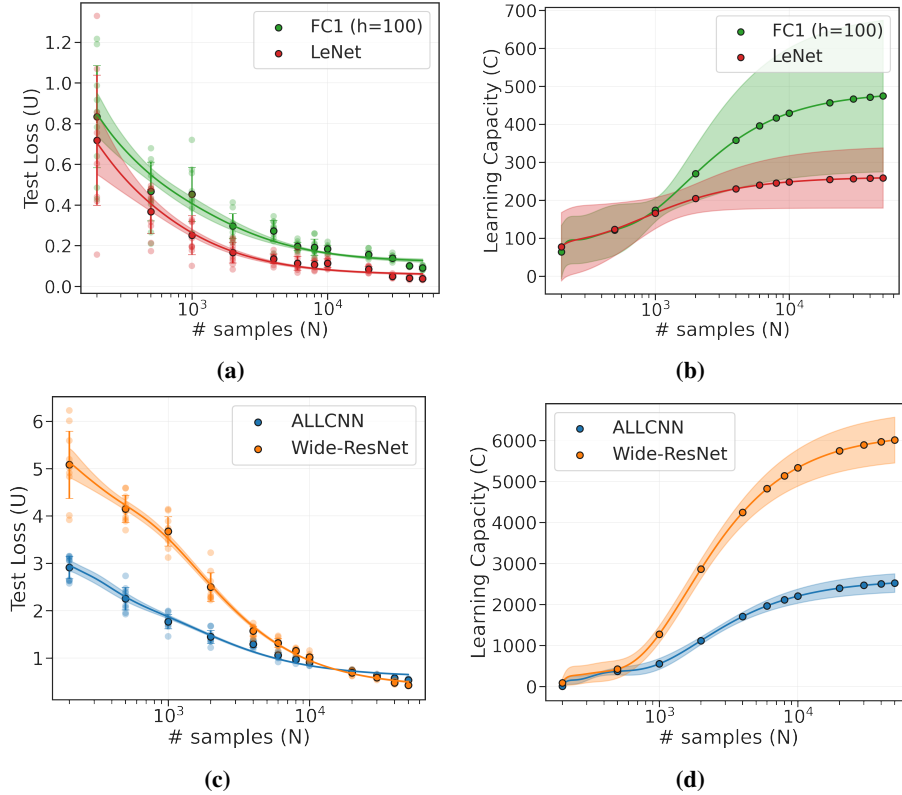


Figure 8: (a,c) show the average energy (\bar{U}) as a function of the sample size N for a one-hidden-layer fully-connected network with 100 neurons and LeNet on MNIST and the ALLCNN and Wide-ResNet on CIFAR-10 (10-class classification in this case). (b,d) shows the learning capacity (\bar{C}) estimated by fitting a seventh-order polynomial to \bar{U} with constraints on it being monotonically decreasing. Since we know that the learning capacity is monotonically increasing, the fit for the average energy should be concave, this adds an additional constraint on the second derivative being negative. These constraints are implemented using `lmfit`⁵⁸. In general, we observe that the learning capacity saturates at both small and large sample sizes; the saturated values and the transition thresholds are different for different architectures and datasets.

Remark 2 (Freezing phenomena in disordered systems). For a free particle with p degrees of freedom confined to a volume, one can calculate the log-partition function exactly to obtain the classical equipartition theorem it has $k_B T/2$ energy for each degree of freedom. The heat capacity \bar{C} of such a free particle is equal to exactly $p/2$. As Lamont and Wiggins discuss¹, in many physical systems, the heat capacity is not as large as $p/2$. Indeed our discussion of singular models in §2.2 suggests that for machine learning models with symmetries, the learning capacity is always smaller than half the number of parameters. In statistical physics, this deviation from the equipartition theorem is well-studied. At very high temperatures, the degrees of freedom in a system can become irrelevant and therefore stop contributing to the heat capacity. Similarly at very low temperatures, there may not be sufficient energy to populate all energy levels and this again leads to a deviation. In physical systems, such freezing can also occur at intermediate temperatures.

We noticed such freezing phenomena for the learning capacity of typical machine learning models when we analytically differentiated polynomial fit to the average energy \bar{U} . We therefore fit a sigmoid

$$\bar{C}(N) = \frac{a}{1 + \exp(-c \log N + b)} \quad (16)$$

where the coefficients a, b, c are to be determined and N is the independent variable. One may think of the coefficient a as the maximal learning capacity of the model with $N \rightarrow \infty$. Just like [8] we expect this to be equal to the number of parameters. We can now deduce an analytical model for $\bar{U} = -\int dN \bar{C}/N^2$ which can be integrated to yield a symbolic formula in terms of the unknown coefficients and the hypergeometric function ${}_2F_1$:

$$\bar{U} = \frac{ae^{(c-1)\log N + bc} {}_2F_1\left[1, \frac{c-1}{c}, 2 - \frac{1}{c}, -e^{(b+\log N)c}\right]}{c-1} + \text{constant}.$$

We fit this expression to the recorded data using the Levenberg-Marquardt algorithm and obtained accurate fits with small uncertainties. This also indicates that the sigmoid-like curve for the learning capacity is a reasonable assumption. Using this technique, we can also circumvent the need to choose sensitive hyper-parameters such as the degree of the polynomial, which can cause issues in getting an accurate fit. We found that both polynomial regression and this sigmoid-based technique give similar estimates of the learning capacity for all the experiments in this paper.

B.1 Estimating the learning capacity using Markov chain Monte Carlo (MCMC) methods

The procedure discussed above to estimate the learning capacity is computationally expensive because it requires us to fit many models with different weight initializations, on different sample sets for each sample size N to calculate the average energy \bar{U} . We also investigated a different technique to estimate the learning capacity using Markov Chain Monte Carlo (MCMC) methods that we describe next. The posterior distribution on the weights can be written as

$$p(w; N) = \frac{1}{Z(N)} e^{-N\hat{H}(w)} \varphi(w).$$

using [1] and [2]. Observe that

$$\begin{aligned} U(N) &= -\partial_N \log Z(N) \\ &\approx \frac{1}{Z(N)} (Z(N) - Z(N+1)) \\ &= \frac{1}{Z(N)} \int dw \left(e^{-N\hat{H}(w;N)} - e^{-(N+1)\hat{H}(w;N+1)} \right) \varphi(w) \\ &= \frac{1}{Z(N)} \int dw e^{-N\hat{H}(w;N)} \left(1 - e^{-(N+1)\hat{H}(w;N+1) + N\hat{H}(w;N)} \right) \varphi(w) \\ &= \int dw \varphi(w) \frac{e^{-N\hat{H}(w;N)}}{Z(N)} (1 - p_w(y_{N+1} | x_{N+1})) \\ &\approx \frac{1}{m} \sum_{i=1}^m (1 - p_{w^{(i)}}(y_{N+1} | x_{N+1})) \end{aligned} \quad (17)$$

where $w^{(i)}$ are samples from a Markov chain that draws samples from $p(w; N)$ and that is why we can approximate the integral using the m samples. We can also calculate an average version of this expression to get

$$\bar{U}(N) = \frac{1}{m} \sum_{i=1}^m \mathbb{E}_{(x,y)} [1 - p_{w^{(i)}}(y | x)].$$

This expression is an alternative to [13] with the key difference that we are drawing samples from the posterior $p(w; N)$ using a Markov chain instead of the leave-one-out cross-validation procedure in [13]. This new expression is computationally more convenient because we only need to run one MCMC chain to draw all the samples. We implement the MCMC chain using stochastic gradient Langevin dynamics (SGLD)⁵⁹.

The learning capacity $C = -N^2 \partial_N U$ depends on the derivative of U which allows us to calculate

$$\begin{aligned} -N^{-2} \bar{C} &= \partial_N \bar{U} = \bar{U}(N+1) - \bar{U}(N) \\ &\approx \frac{1}{m} \sum_{i=1}^m \mathbb{E}_{(x,y)} \left[p_{w_N^{(i)}}(y | x) - p_{w_{N+1}^{(i)}}(y | x) \right]. \end{aligned}$$

In principle, we should run two Markov chains, one that draws samples $w_N^{(i)}$ and another, completely independent one, that draws samples $w_{N+1}^{(i)}$. Since we need to estimate $\bar{C}(N)$ for many different values of the sample size N , this would again require us to implement many different Markov chains. In practice, we implement a coarse approximation of this procedure, where we think of the number of samples N as a parameter that varies with time and set

$$-N^{-2}\bar{C} \approx \frac{1}{m} \sum_{i=1}^m \mathbb{E}_{(x,y)} \left[p_{w_t^{(i)}}(y|x) - p_{w_{t+\Delta t}^{(i)}}(y|x) \right] \quad (18)$$

where t denotes the number of MCMC updates and Δt is the interval after which we increase the sample size by one (in practice, this involves simply adding a new sample, or a few samples, to the dataloader and waiting until the draws from the Markov chain become uncorrelated, e.g., for a few epochs). In practice, we do not sweep all values of N but instead sweep through a set of sample sizes (but still use these finite difference estimates of the thermodynamic quantities). This construction is inspired from⁶⁰ which estimates the thermodynamic length, a quantity that characterizes the distance between two equilibrium states by endowing the state-space with a Riemannian metric and calculating the length of a path that joins the end points using quasi-static transformations.

This MCMC approach allows us to estimate the average energy \bar{U} and learning capacity \bar{C} using a single Markov chain, but one where the number of samples N increases with time t .

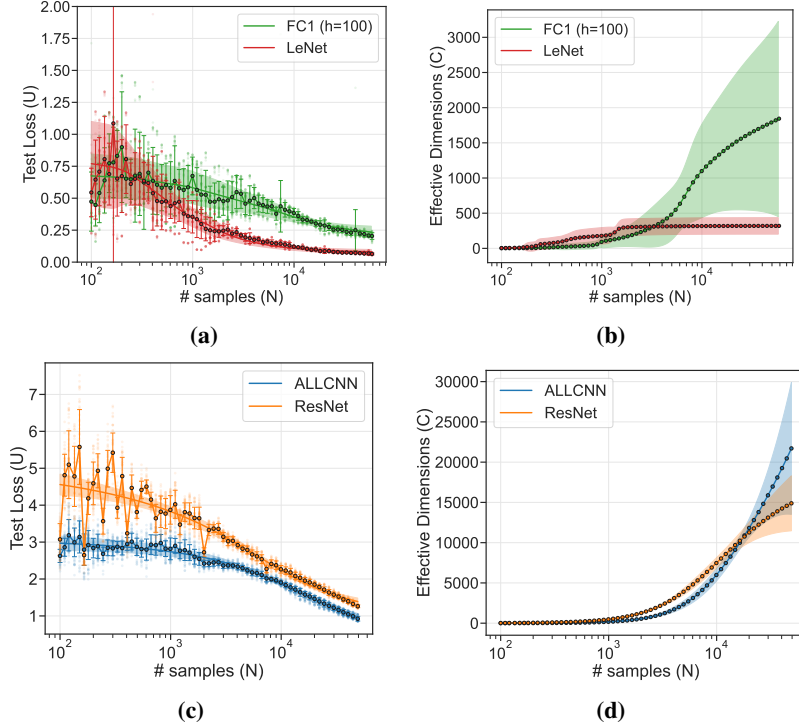


Figure 9: (a,c) show the estimate of the average energy $\bar{U}(N)$ for different architectures, for MNIST and CIFAR-10 datasets respectively. The numerical estimates of the average energy are higher than those in Fig. 2 and we also see marked jitter on these curves. This noise in the derivative translates to much higher estimates of the learning capacity \bar{C} in (b,d) than those in Fig. 2. Even in this case, some of the broad patterns are preserved, e.g., the learning capacity is a tiny fraction of the number of weights, it saturates at both small and high sample sizes; there is no low-temperature saturation for CIFAR-10.

As Fig. 9 shows, the estimates of the thermodynamic quantities using this procedure exhibit the same trends that we have discussed in the main paper in Fig. 2. The effective dimension is much smaller than the number of weights in these models. The MCMC-based estimate of the learning capacity is much larger. This can be explained by the large derivative of the estimate of \bar{U} in Fig. 9 (a,c). It is interesting to note that the MCMC-based estimate of \bar{U} is also larger than the corresponding one using SGD in Fig. 2. We suspect that this is because of the sharper posterior of SGD than stochastic gradient Langevin dynamics; this is consistent with the fact that in practice, SGLD often

obtains poorer test errors than SGD. There is another way to interpret the results of this experiment: the MCMC-based learning capacity estimates are higher than those using SGD discussed in the main paper. While we have focused on the utility of the learning capacity for model selection across architectures and datasets, we see some evidence here that the learning capacity can also distinguish between different training algorithms (which affect the kinds of solutions found at the end of training). Again, it is reassuring that *smaller* the learning capacity, better the test loss.

C Details of the experimental setup

Datasets We use MNIST⁹ and CIFAR-10¹³ datasets for our experiments on image classification, and binary-class (miniboone, higgs, numerai) and multi-class datasets (covertype, jannis, connect) for experiments using tabular data; see⁶¹ for a description of how these datasets were curated. For MNIST, we set up a binary classification problem (even digits vs. odd digits). The synthetic data was created by sampling $d = 200$ dimensional inputs for at most $N = 50,000$ from a Gaussian distribution whose covariance has eigenvalues that decay as $\lambda_i = e^{-\kappa i}$ (i.e., larger the slope κ , more low-dimensional the inputs) and labeled these inputs using a random teacher network with one hidden layer (1000 neurons, 2 classes).

Architectures We use the original LeNet-5 network (convolutional layers and linear layers with tanh as the activation function) and MLPs (one layer, different numbers of hidden neurons and ReLU non-linearity) to train on the MNIST dataset and the synthetic dataset. We use a Wide-ResNet¹² with a depth of 10 layers and a widening factor of 8 and the ALLCNN network¹⁰ to train on CIFAR-10. For the tabular datasets, we use random forest-based (RFs) and k -NN (k -nearest neighbor) classifiers. We set the total estimators in RF to be 1000, and use the gini criterion for splitting. We do not restrict the maximal depth of each tree, this entails that each node will expand until the leaves are pure (i.e., all samples in the leaf are from the same class). For the k -nearest neighbor classifiers, we set the number of neighbors to be 10.

Training Procedure We use all samples from the training set and record the average energy for 14 different values of N in the set [200, 400, 600, 800, 1000, 2000, 4000, 6000, 8000, 10000, 20000, 30000, 40000, 50000]. The MCMC-based estimates are much more inexpensive computationally and we therefore sampled 63 different values of N uniformly on a log-scale between 100 and 50,000. No data augmentation is performed on MNIST, CIFAR-10 and synthetic data. We only normalize the images of each dataset with mean and standard deviation. As discussed in Appendix B, we used $k = 5$ cross-validation folds to estimate the average values of U, C . We train all models with SGD and Nesterov’s momentum (with coefficient 0.9), and a learning rate schedule that begins with a value of 0.5 and decays using a cosine curve for one cycle⁶². We train for 200 epochs for all datasets and models. The batch size is set to be 64 for all experiments.

We will now describe how we add samples incrementally while running SGLD. Suppose we start from some initial sample size N_1 and would like to change it to N_2 . We first split the N_1 samples into $k = 10$ equal-sized folds and run $k = 10$ Markov chains in parallel on these folds; these Markov chains are run completely independent of each other. After 20 epochs, we add $(N_2 - N_1)/k$ samples into each of the k Markov chains’ dataset; we assume that the Markov chain reaches an equilibrium after 20 epochs of training on this expanded dataset with $((k - 1)N_2)/k$ samples and draw 10 samples $w^{(i)}$ from the last 10 epochs to calculate the expressions in [17] and [18].

D Further experimental results for random forests

We saw in the main text (see Fig. 6b) that the random forest models do not exhibit freezing of the learning capacity at large samples. This is an indicator of the powerful function approximation capabilities of these models. Roughly speaking, this is an attempt to think of the number of leaves in a random forest as being equivalent to the number of weights in a neural network. Both quantities describe the number of degrees of freedom available to their respective models and training corresponds to allocating these degrees of freedom to fit the data. Since we saw that the learning capacity of neural networks exhibits freezing at large sample sizes, we should also expect this behavior for random forests. We set the total number of trees in the forest as 1,000 (same as the original experiment) but restricted the maximal amount of leaf nodes to 100 (in the original experiment, each node is split until the leaves are pure). As shown in Fig. 10a and Fig. 10b, the learning capacity of random forest models exhibits freezing at large sample sizes when the number of leaf nodes in each tree is restricted.

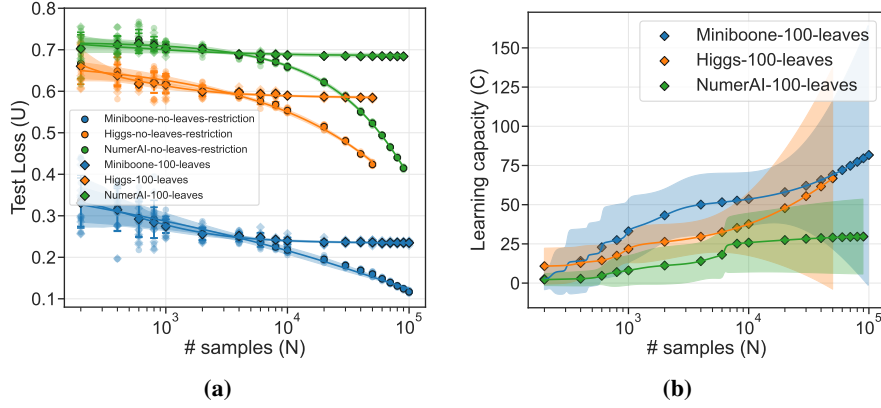


Figure 10: (a) shows the average energy for random forest models on different datasets (different colors) with (diamonds) and without (circles) a restriction on the number of leaves in each tree. Although the average energy is quite similar for both methods at small sample sizes, as expected models without any restrictions continue to decrease the average energy at large sample sizes. This corresponds to the saturation of the learning capacity in (b); contrast this with Fig. 6b where the learning capacity is growing quickly even at large sample sizes.

We therefore believe that freezing is a general phenomenon for machine learning models with a fixed number of degrees of freedom.